Supporting Information

Pulse laser-induced fragmentation of carbon quantum dots: a structural analysis

Han-Wei Chu,[a] Ju-Yi Mao,[a] Chia-Wen Lien,[a] Pang-Hung Hsu,[a] Yu-Jia Li,[b] Jui-Yang Lai,[b] Tai-Chia Chiu,[*c] and Chih-Ching Huang[*a,d,e]

[a]Department of Bioscience and Biotechnology, National Taiwan Ocean University, Keelung, 20224, Taiwan

[b]Institute of Biochemical and Biomedical Engineering, Chang Gung University, Taoyuan, 33302, Taiwan

[c]Department of Applied Science, National Taitung University, Taitung, 95092, Taiwan

[d]Center of Excellence for the Oceans, National Taiwan Ocean University, Keelung, 20224, Taiwan

[e]School of Pharmacy, College of Pharmacy, Kaohsiung Medical University, Kaohsiung, 80708, Taiwan

Correspondence: Tai-Chia Chiu, Department of Applied Science, National Taitung University, 369, Sec. 2, University Rd, Taitung, 95092, Taiwan; E-mail: tcchiu@nttu.edu.tw; Chih-Ching Huang, Department of Bioscience and Biotechnology, National Taiwan Ocean University, 2, Pei-Ning Road, Keelung, 20224, Taiwan; E-mail: huanging@ntou.edu.tw

Table S1. Elemental analyses and Zeta potentials of the as-prepared CA-CQDs, AC-CQDs, and Spd-CQDs.

	Elemental compositions (wt%)				Zeta potential (mV; n = 5)
	C	O	N	H	
CA-CQDs	39.31	49.82	ND[a]	5.04	–35.3 ± 5.6
AC-CQDs	41.25	37.86	11.82	4.74	–28.3 ± 7.8
Spd-CQDs	39.21	8.80	12.59	11.02	+34.5 ± 4.2

[a]Not Detected

Table S2. Elemental analysis of AC-CQDs by SEM-EDS after treating with different laser shots.

Atom (% mass)	0 shots	100 shots	1000 shots	5000 shots
carbon	41.54	42.19	43.57	44.63
nitrogen	10.37	10.02	8.95	8.45
oxygen	48.09	47.79	47.49	46.92

Table S3. Identification of Spd-CQDs' selected fragments from LDI-MS data.

Monoisotopic mass			
144.914	Chemical formula	Theoretical *m/z*	Mass accuracy (ppm)
1	CCl_3N_2	144.913	9
2	$C_2H_2Cl_3N$	144.925	78
3	C_2Cl_3O	144.901	86
4	$C_3H_4Cl_3$	144.938	165
Monoisotopic mass			
150.944	Chemical formula	Theoretical *m/z*	Mass accuracy (ppm)
1	C_3ClO_5	150.943	7
2	$C_2ClN_2O_4$	150.955	73
3	C_7ClO_2	150.959	99
4	$CClN_4O_3$	150.966	146
Monoisotopic mass			
166.882	Chemical formula	Theoretical *m/z*	Mass accuracy (ppm)
1	$CHCl_4N$	166.886	24
Monoisotopic mass			
184.930	Chemical formula	Theoretical *m/z*	Mass accuracy (ppm)
1	$C_3HCl_2NO_4$	184.928	9
2	$C_2HCl_2N_3O_3$	184.939	51
3	$C_4H_3Cl_2O_4$	184.941	59
4	C_7HCl_2NO	184.944	73

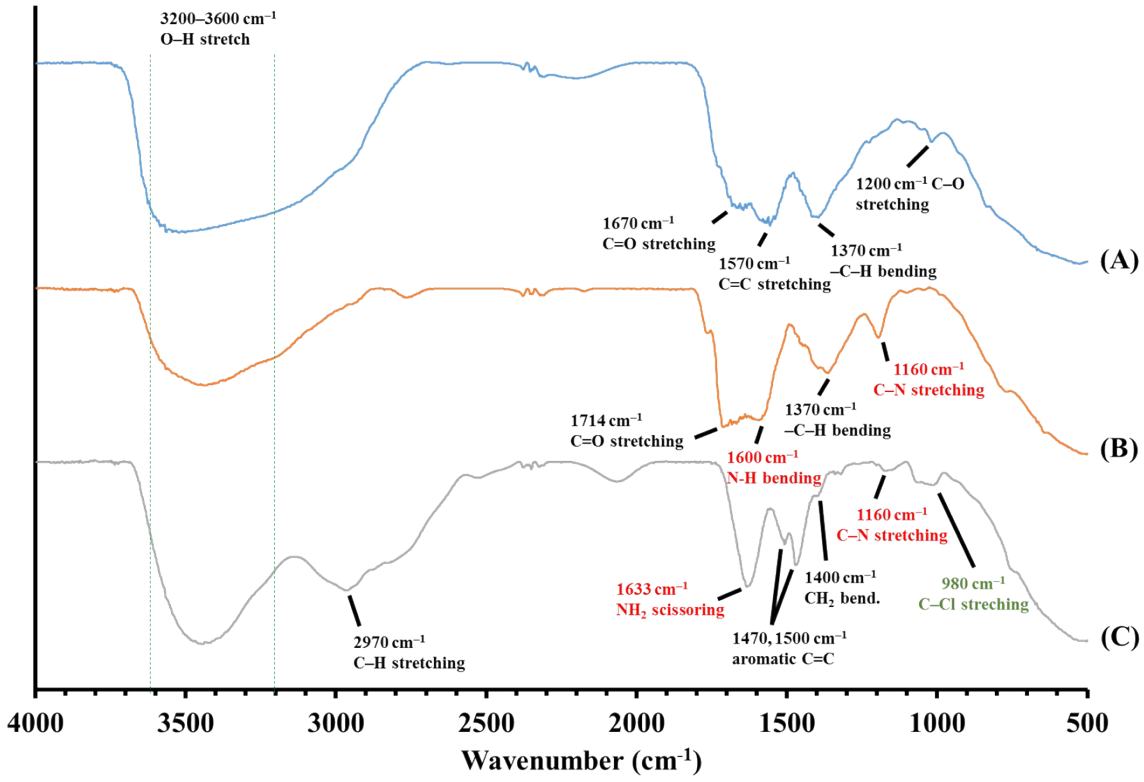

Figure S1. FTIR spectra of (A) CA-CQDs, (B) AC-CQDs, and (C) Spd-CQDs.

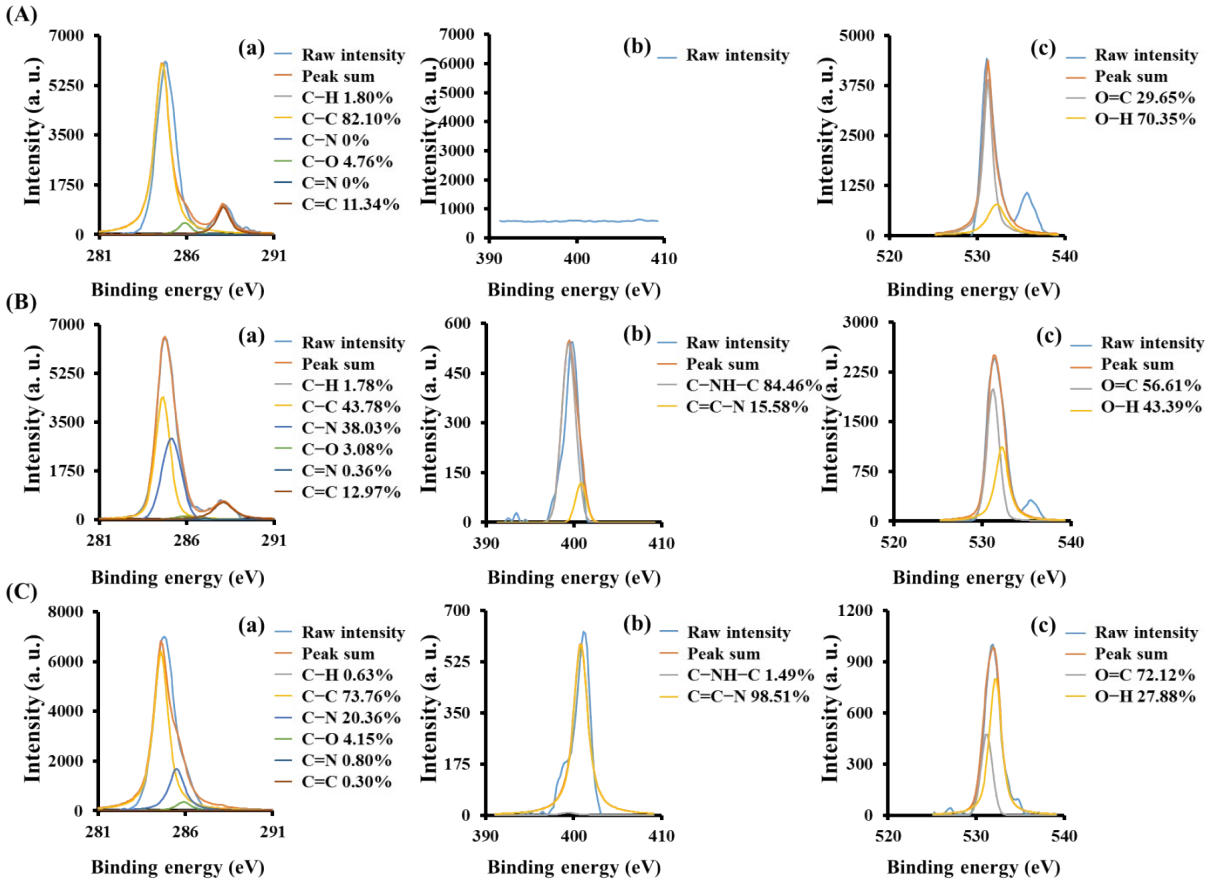

Figure S2. Deconvoluted (a) C 1s, (b) N 1s, and (c) O 1s XPS spectra of (A) CA-CQDs, (B) AC-CQDs, and (C) Spd-CQDs.

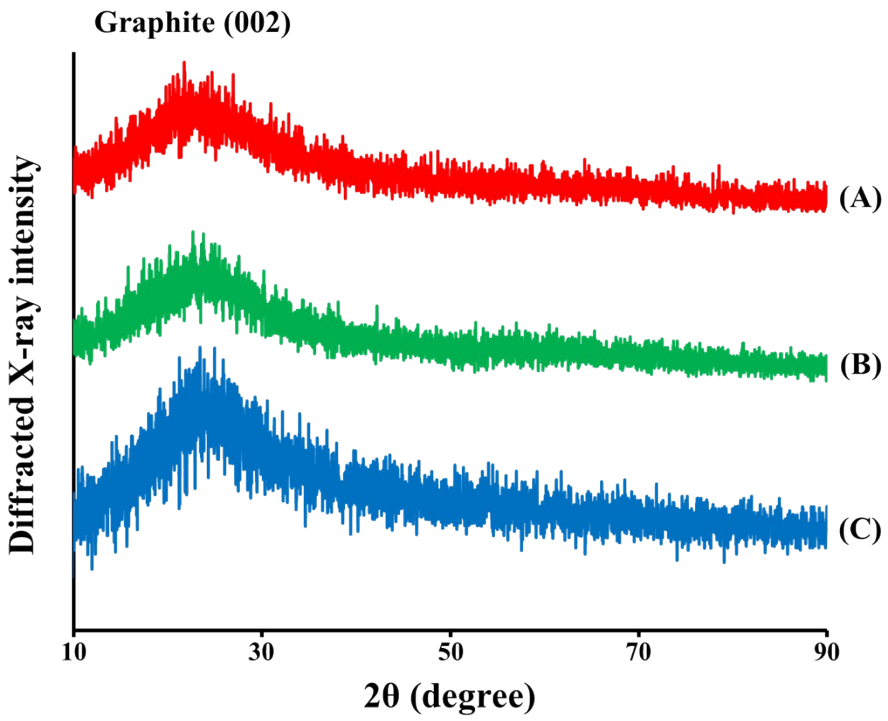

Figure S3. XRD spectra of (A) CA-CQDs, (B) AC-CQDs, and (C) Spd-CQDs.

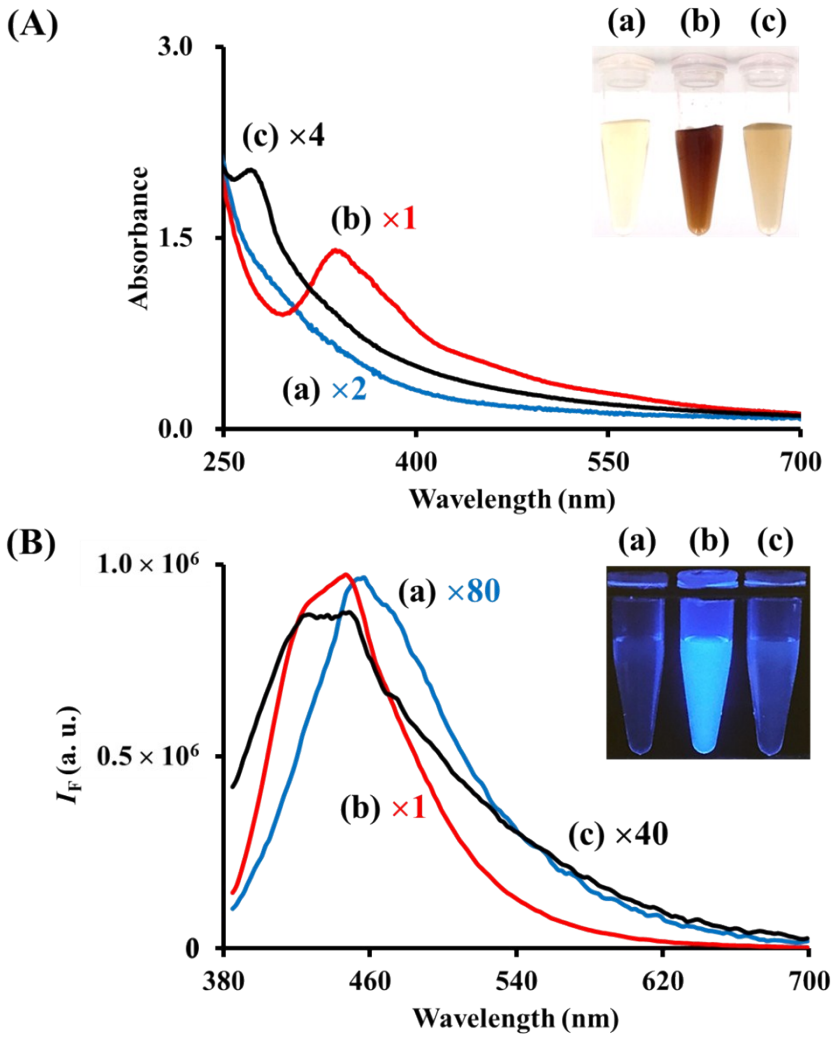

Figure S4. (A) UV-Vis absorption and (B) fluorescence spectra of (a) CA-CQDs, (b) AC-CQDs, and (c) Spd-CQDs in 5 mM sodium phosphate buffer (pH 7.4). The concentration of each CQD is 50 μg mL^{-1} and 10 μg mL^{-1} for the UV-Vis absorption and fluorescence measurements, respectively. Insets in panels (A) and (B): photographs of the corresponding solutions (A) before and (B) during excitation with a UV lamp (365 nm). Fluorescence spectra of CQDs were recorded at an excitation wavelength of 365 nm. The fluorescence intensities (I_F) are plotted in arbitrary units (a. u.).

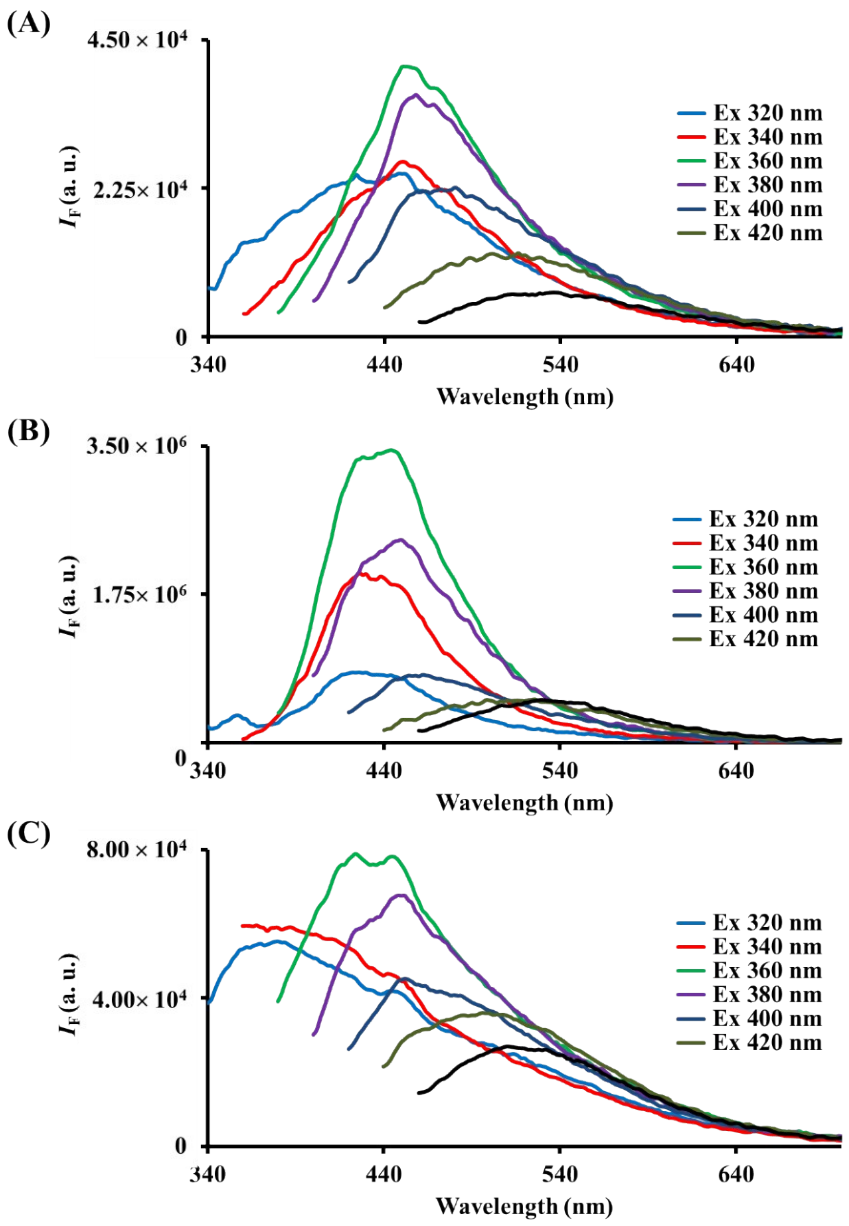

Figure S5. Fluorescence spectra of (A) CA-CQDs, (B) AC-CQDs, and (C) Spd-CQDs under different excitation wavelengths (in 20-nm increments from 320 to 440 nm) in 5 mM sodium phosphate buffer (pH 7.4).

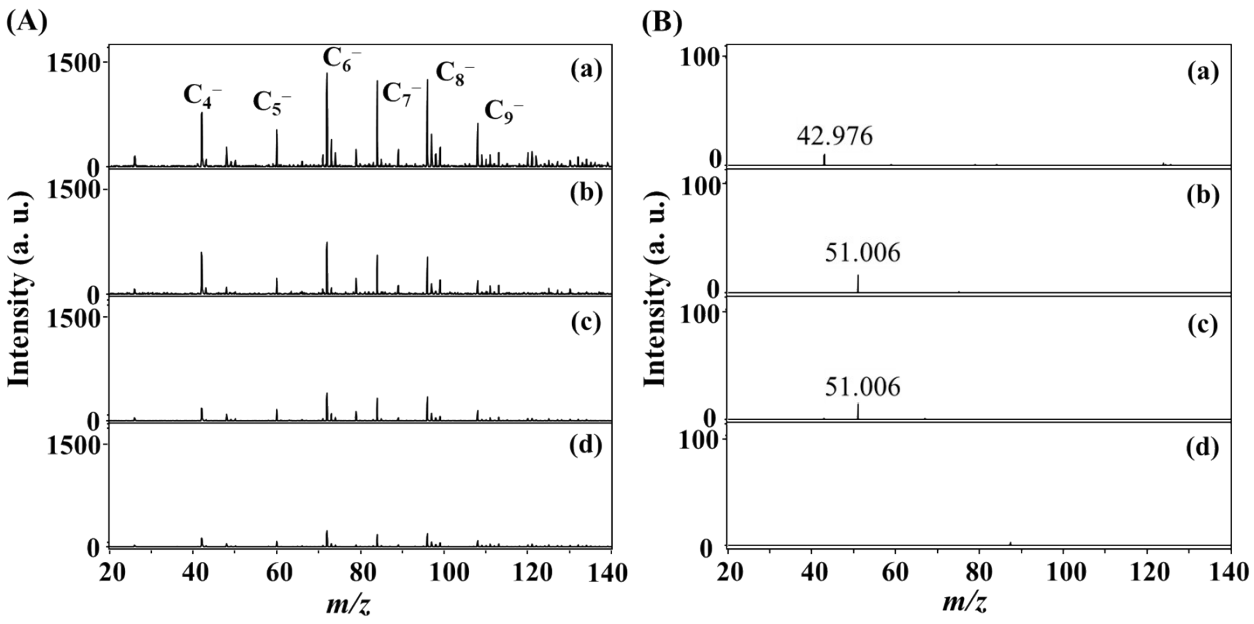

Figure S6. LDI-MS spectra of the stainless steel 384-well MALDI target plate (A) without and (B) with taped-on aluminum foil. MS spectra were recorded for the (a) 1st, (b) 4th, (c) 7th and (d) 10th 500 pulsed laser shots with a laser density of 12.30 J cm^{-2}. Peak intensities are plotted in arbitrary units (a. u.).

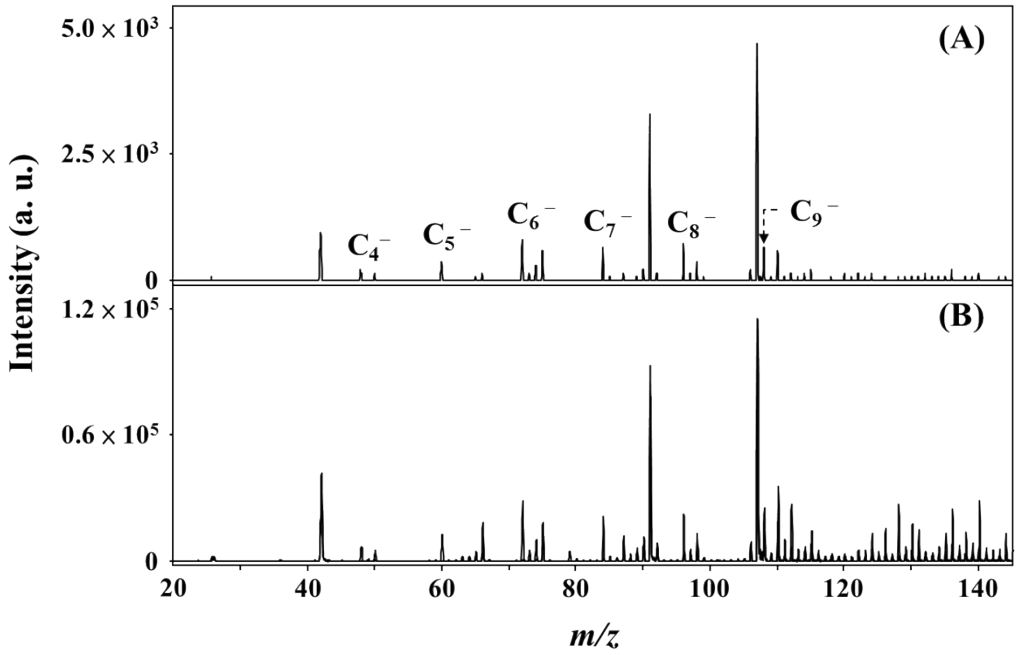

Figure S7. Mass spectra of AC-CQDs (0.4 mg mL^{-1}) on aluminum foil, recorded at a laser density of (A) 11.59 J cm^{-2} and (B) 14.80 J cm^{-2}. 500 pulsed laser shots were applied to five random positions on the MALDI target. Peak intensities are plotted in arbitrary units (a. u.).

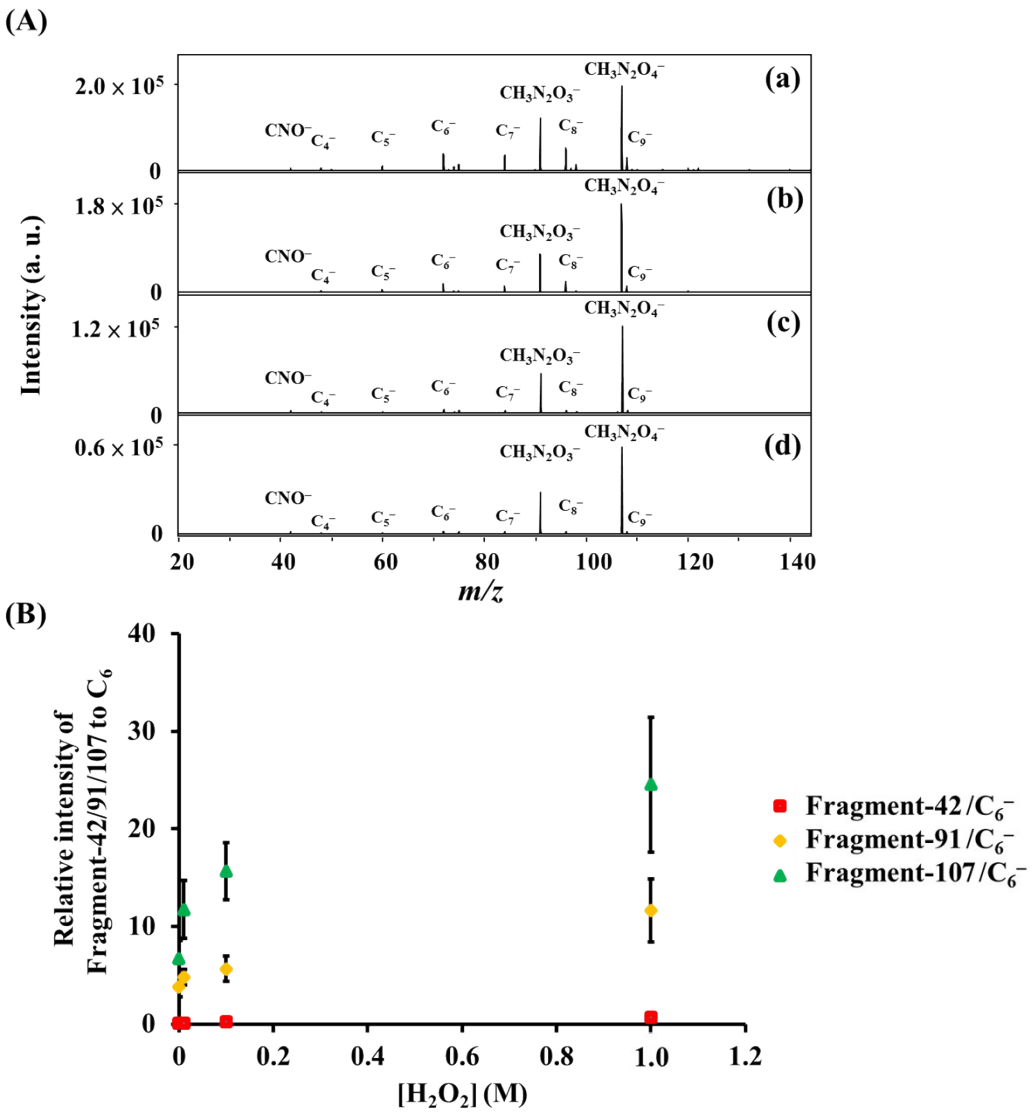

Figure S8. (A) Mass spectra of (a) AC-CQDs (0.4 mg mL^{-1}) and (b–d) after treatment with H_2O_2 (b) 0.01 M, (c) 0.1 M, and (d) 1.0 M for 2 h. (B) Signal intensities of Fragment-42, Fragment-91 and Fragment-107, relative to $[C_6]^-$, plotted with respect to the concentration of H_2O_2 (0–1.0 M). The error bars in (B) represent the standard deviations from five repeated experiments. Other conditions were the same as those described in Figure 2.

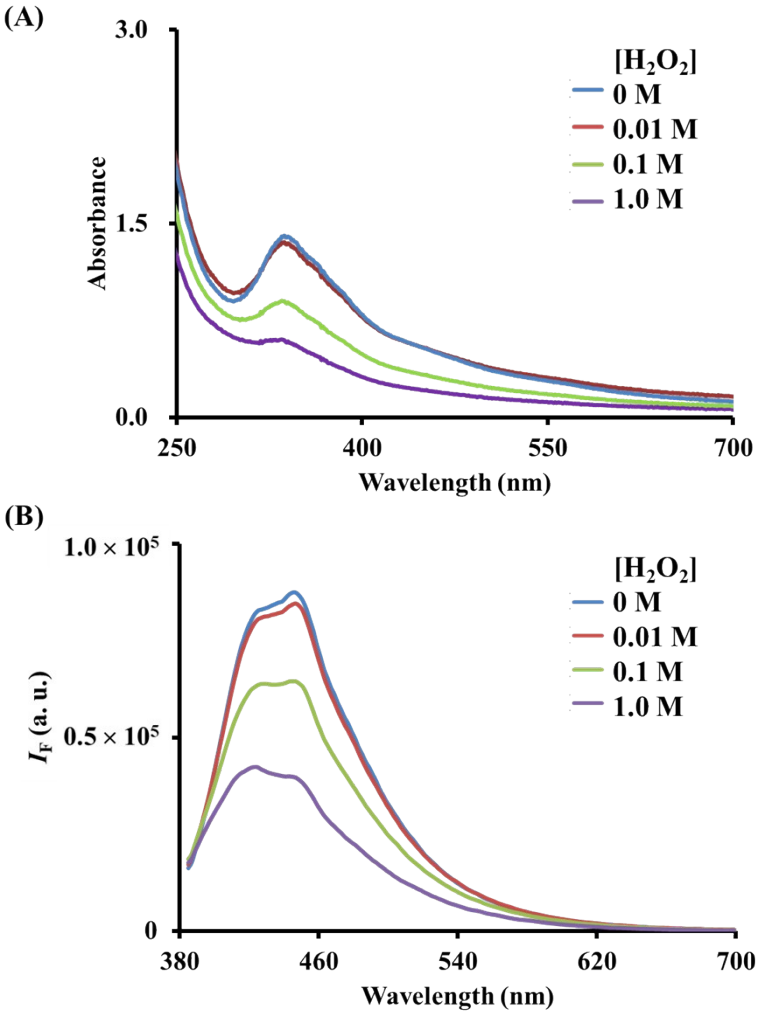

Figure S9. (A) UV-vis absorption and (B) fluorescence spectra of AC-CQDs (10 μg mL^{-1}) in DI water after treatment with H_2O_2 (0–1.0 M). Fluorescence spectra of CQDs are recorded at an excitation wavelength of 365 nm. The fluorescence intensities (I_F) are plotted in arbitrary units (a. u.).

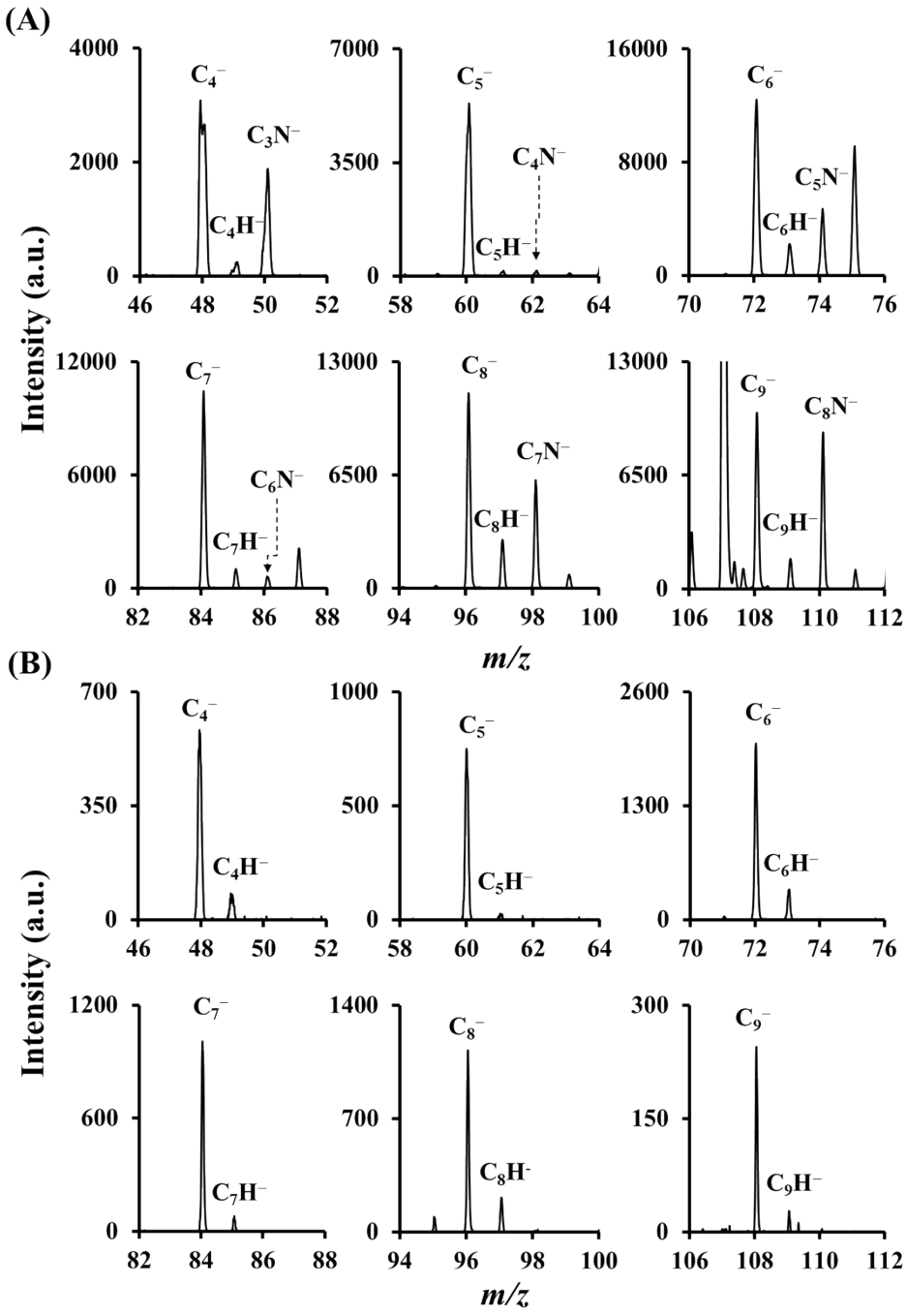

Figure S10. LDI-MS spectra of (A) AC-CQDs (0.4 mg mL^{-1}) and (B) CA-CQDs (0.4 mg mL^{-1}) at different *m/z* regions obtained from the first 500 shots with a laser energy density of 12.30 J cm^{-2}. Peak intensities are plotted in arbitrary units (a. u.).

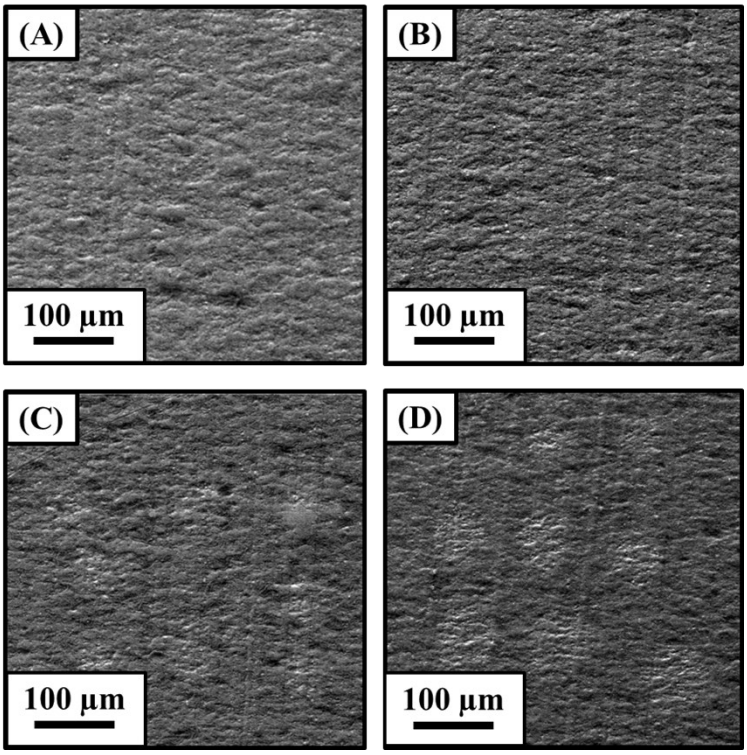

Figure S11. SEM images of AC-CQDs (0.4 mg mL^{-1}) (A) before and (B–D) after (B) 100 shots, (C) 1000 shots and (D) 10000 shots. A 3×3 array was patterned by pulse laser irradiation for each shot condition.

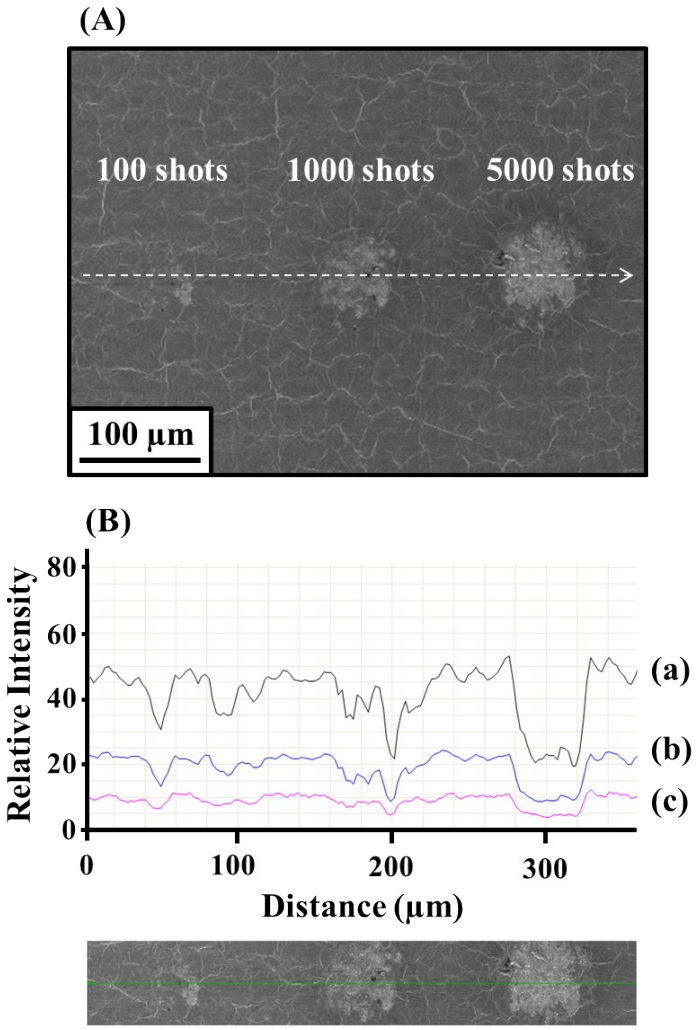

Figure S12. (A) SEM image of AC-CQDs after treatment with different laser shots. (B) EDS line scan of (a) carbon, (b) oxygen and (c) nitrogen signals across the ablated spots.

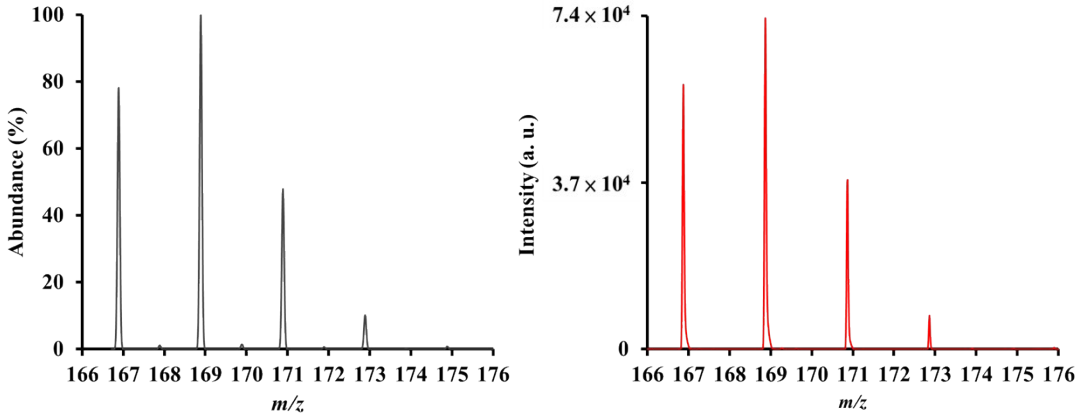

Figure S13. Comparison of predicted (left, gray) and observed (right, red) isotopic distributions of chlorine-based fragments ($CHCl_4N$) in the LDI mass spectra of Spd-CQDs.